Nonlinear Response Assessment of an Instrumented Building in Acapulco

W. Morales-Avilés*, D. Murià-Vila & S. Loera-Pizarro
Instituto de Ingeniería, UNAM, Ciudad Universitaria, Coyoacán, 04510 México, D.F.

**Now at Bundesanstalt für Geowissenschaften und Rohstoffe (BGR), Stilleweg 2, 30655 Hannover, Germany.*

SUMMARY:
Given the possibility of the occurrence of a strong earthquake at the Guerrero seismic gap in Acapulco, Mexico, a 17-story reinforced concrete building was instrumented, in order to assess its response to strong motion seismic events. This paper presents the structural responses of the building obtained from a nonlinear step-by-step analysis using the program Ruaumoko. The analysis was conducted with a synthetic record that simulates a strong motion event (Mw=8.2) whose epicentre is located in the Guerrero seismic gap. In the calibrated numerical model, the soil-structure interaction effects and the hysteretic behavior of the structural elements have been considered. The nonlinear response of the building was evaluated by comparing and discussing the global and local responses. The envelopes of story drift ratios, story shears, seismic coefficients demands and the corresponding design parameters were compared. Further, the structural damage assessment was performed by calculating the damage index of the structural elements. Some conclusions are presented.

Keywords: Nonlinear response, Instrumented buildings, Guerrero seismic gap, Acapulco building code

1. INTRODUCTION

Because of high seismic hazard at the Guerrero Coast and the high seismic potential of the Guerrero seismic gap (Singh and Mortera, 1991), and due to the importance of evaluating the nonlinear behavior of structures subjected to strong earthquakes, the *Instituto de Ingeniería-Universidad Nacional Autónoma de México* (II-UNAM) instrumented a new, regular and almost symmetrical 17-story reinforced concrete building in Acapulco city at the end of the year 2000.

The floor plan of the building is approximately square and its height is about 66 m (Fig. 1.1). The structural system consists of reinforced concrete moment frames with reinforced concrete walls. Masonry walls were considered as non-structural elements. The foundation type consists of reinforced concrete embedded box supported by piles of reinforced concrete. Plan dimensions of foundation are 32.9 m in the longitudinal (L) component and 37.5 m in transverse (T) component. The site geology is characterized as soft and compressible clays (RCMACA, 2002).

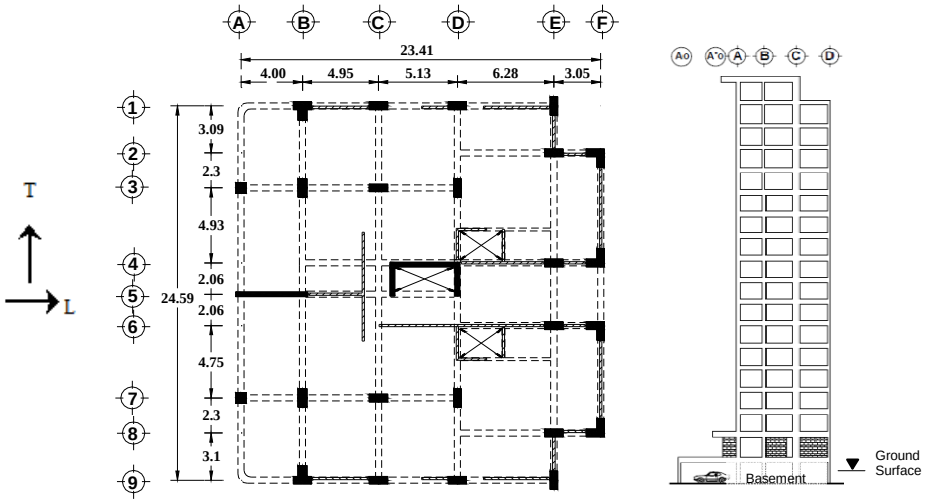

Figure 1.1. Typical structural floor plan and frame through axis 3 and 7 in L component (dimensions in m)

The building has 21 uniaxial well distributed accelerometers and a triaxial field instrument (Alcántara *et al.*, 2002). More than 100 small size earthquakes have been recorded in the building; for this paper, the most intense earthquake recorded (01-1) has been selected. Earthquake 01-1 occurred on October 8, 2001 with a moment magnitude of 6.1. The epicentre of earthquake 01-1 was located approximately 44 km from the building. The peak ground acceleration (L component) and Arias intensity were 77.5 cm/s^2 and 16 cm/s, respectively (Murià-Vila *et al.*, 2004).

The Ruaumoko software version 1998 (Carr, 1998) was used to model the building and estimate its linear and nonlinear behavior. The frequencies and modal shapes of the linear model were calibrated with experimental data obtained from ambient vibration measurements, and seismic event 01-1 recorded in the building.

This paper presents the evaluation of the nonlinear response by comparing and discussing the global and local responses obtained from a step-by-step analysis using a synthetic record. The envelopes of the story drift ratios, story shears, seismic coefficient demands and the corresponding design parameters are compared. The structural damage assessment was performed by calculating the damage index of the structural elements.

2. SYNTHETIC GROUND MOTION

The synthetic time history for the nonlinear analysis was calculated based on empirical Green's functions (Ordaz *et al.*, 1995). This method uses small events as seed motions to obtain scaled ground motions at certain magnitudes. In this study, the ground motions from seismic event 01-1 recorded at the field station of the building were considered, and a total of 100 simulations were calculated.

One significant synthetic time history for the nonlinear analysis has been employed (hereinafter called SIM81). The selection criterion consists of three parts: a) choosing the synthetic record with similar and slightly greater response spectral values than the average spectrum; the average spectrum (5% critical damping) was calculated from the entire set of simulations. b) The motion with less uncertainty in the estimation of the moment magnitude and stress drop. c) The motion with similar spectrum to the local building code design spectrum.

It is worthwhile mentioning that there are some uncertainties in determining the stress drop of both the seed and target motions, as well as the determination of seismic moment of the seed accelerograms. Furthermore, another source of uncertainty is related to scaling weak accelerograms to very strong time histories. Because of these arguments, the development of synthetic time histories should be

considered with caution.

For this study, the synthetic ground motion SIM81 was selected based on the selection criterion indicated above, and also because its maximum spectral amplitudes occurred at periods less than 1.8 s. The identified dominant period of the site (determined with the waveforms recorded at field station) ranged from 1.26 to 1.40 s (Murià-Vila *et al*. 2004). The acceleration time history of SIM81 and its response spectrum are shown in Figs. 2.1 and 2.2, respectively.

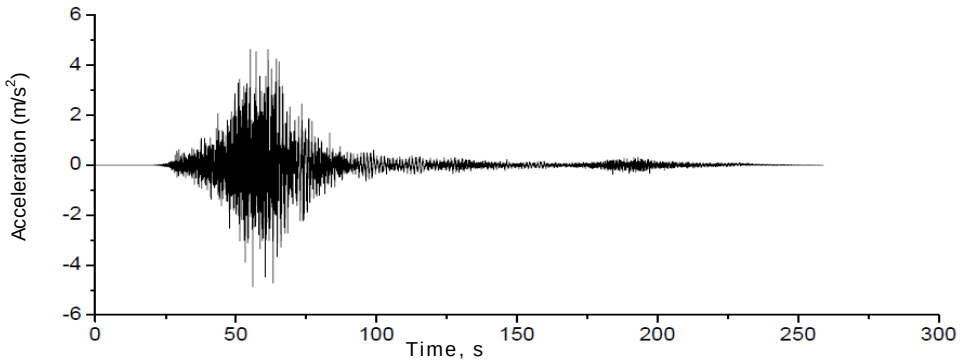

Figure 2.1. Ground acceleration time history SIM81

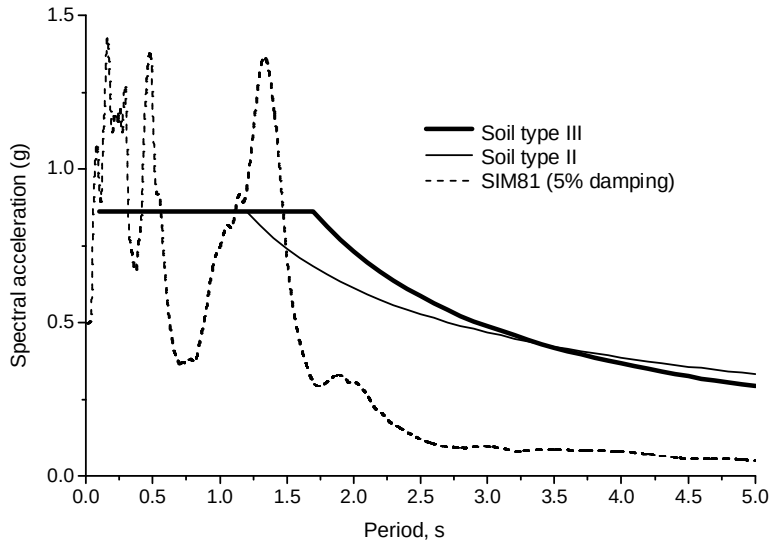

Figure 2.2. Acceleration response spectrum of synthetic motion SIM81 and local building code design spectrum (RCMACA, 2002)

3. ANALYTICAL MODELS

To analyze the nonlinear response of the building in L component, it was necessary to have a representative mathematical model. To achieve this aim, the Ruaumoko software (Carr, 1998) was used to develop a two dimensional (2D) model of the building. The 2D model was used for estimating the linear and nonlinear behavior. The Etabs software (Wilson, 2000) was used for developing a three dimensional (3D) linear model.

3.1 Linear Model

The analytical-linear planar model was calibrated with the 3D model, and with the experimental frequencies and modal shapes obtained from the ambient vibration measurements and from the

seismic event 01-1 recorded in the building (Taborda *et al*., 2002 and Murià-Vila *et al*., 2004).

The modal frequencies obtained from the 2D and 3D linear models are very close to the values obtained from the motion recorded at the building (Table 3.1). General assumptions of the linear model are listed below:

1. A rigid floor diaphragm with infinite in-plane stiffness.
2. The real distribution of masses.
3. Soil-structure interaction (SSI) effects were considered by using the translational and rotational stiffness calculated with experimental data (Murià-Vila *et al*., 2004).
4. A reduction factor of 0.50 on rigid-zone in the frames joints.
5. The modulus of elasticity of concrete and masonry walls for low stresses.
6. Gross cross sections of structural elements (uncracked elements) were used.
7. The effective flange width for beams type L or T (NTC-Concreto, 2004) was taken into account.
8. For 2D models, the influence of rigid out of plane elements has been considered by using spring members (Morales-Avilés, 2005).

The 2D model consists of a set of nine frames (L component of building), which were aligned one after another.

Table 3.1. Modal frequencies obtained from a seismic event, ambient vibration tests and for the 2D model (Ruaumoko) and 3D model (Etabs) for longitudinal direction

Event	Mode No.	Frequencies (Hz)
Ambient vibration VA-011	1	1.17
	2	4.10-4.12
	3	8.01-8.50
Seismic event SI-011	1	1.00
	2	4.07-4.17
	3	7.30-8.00
Ambient vibration VA-021	1	1.07
	2	4.00-4.35
	3	8.10
3D linear model (*Etabs*)	1	0.98
	2	3.53
	3	6.40
2D linear model (*Ruaumoko*)	1	1.00
	2	3.30
	3	6.27

3.2 Nonlinear Model

The nonlinear 2D model of the building was created using the longitudinal linear 2D model as basis. Assumptions 1 to 4 for the linear model are also applicable to the nonlinear model. Additional assumptions made for the nonlinear model are given below:

1. Five percent of critical damping.
2. Sources of overstrength (steel bars, confinement and flange effective width on beams).
3. Initial stiffness of structural elements based on building code from New Zealand (New Zealand Standard, 1999).
4. The simplest form of plastic hinge length, 0.50 of section depth.
5. Masonry walls were not considered due to its low influence in stiffness and strength.

The modified Takeda degrading stiffness hysteresis rule (Otani, 1974) and Li Xinrong hysteresis rule (Li Xinrong, 1995) were defined for the beams and the reinforced concrete columns, respectively. For

reinforced concrete walls, a combination of Kato *et al.* (1983) hysteresis rule and bilinear behavior hysteresis was employed.

In order to determine the best estimate parameters of the hysteresis models, a calibration procedure between experimental and analytical responses was performed. The experimental values are obtained from published results (Salonikios *et al.*, 1999, Shao-Yeh *et al.*, 1976, Tanaka and Park, 1990, and Wang *et al.*, 1975). The comparison of some responses is shown in Fig. 3.1(Morales-Aviles, 2005).

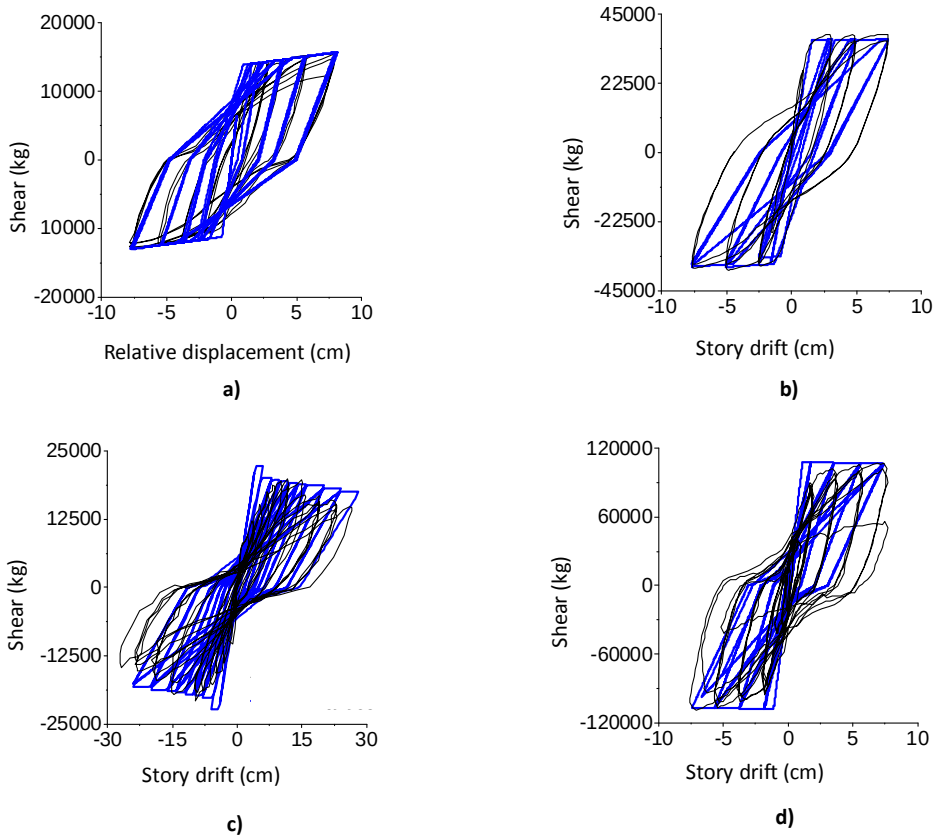

Figure 3.1. Comparison of analytical (blue lines) and experimental (black lines) hysteretic responses for a) beam, b) column, c) concrete wall and d) slender concrete wall

4. NONLINEAR RESPONSE

4.1 Displacement time histories

A comparison between the computed linear and nonlinear displacement time histories is shown in Fig. 4.1. The response is calculated between the roof and the building base. The nonlinear behavior started at approximately 55 s. The maximum nonlinear displacement is almost 50% of the maximum linear displacement. The maximum displacement at the roof of the building was about 32 cm. Permanent displacements occurred after 79 s.

4.2 Base shear time history analysis

The results for the linear and nonlinear base shears, generated in the course of the time history analysis, are shown in Fig. 4.2. The linear and nonlinear responses are similar for the first 48 s. The maximum nonlinear base shear (2,716 t) was 35% of the linear response.

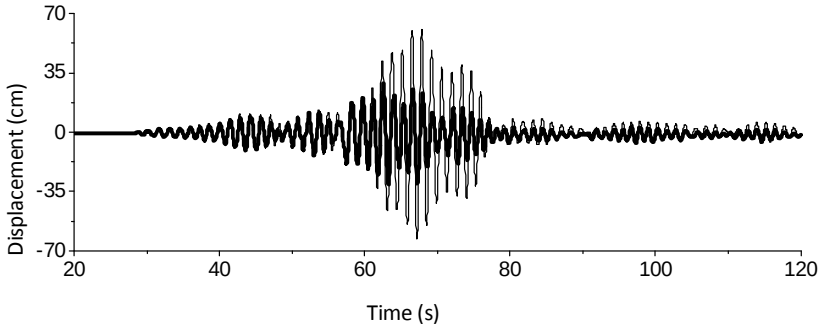

Figure 4.1. Linear (thin lines) and nonlinear (thick lines) relative displacement time history

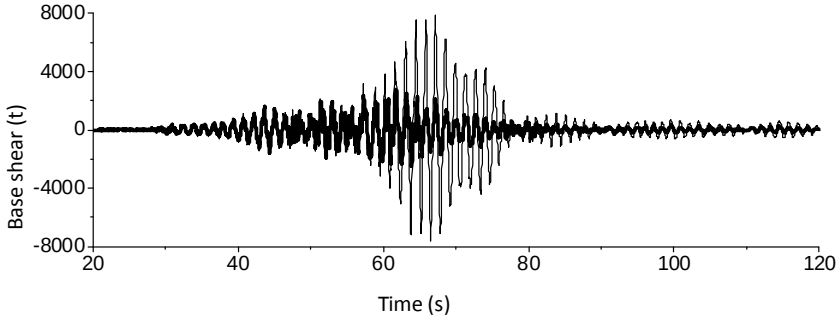

Figure 4.2. Linear (thin lines) and nonlinear (thick lines) base shear time history

4.3 Seismic coefficient

The seismic coefficients (c) from the nonlinear analysis with the synthetic time history SIM81 were calculated. The seismic coefficients were estimated as the ratio between base shear and the total weight of building. In estimating the value of c from the Acapulco building code (RCMACA, 2002), a ductile reduction factor Q=4 and soil type III were used. A maximum seismic coefficient demand of 0.226 was estimated. This value exceeds the seismic coefficient estimated by the local building code (c=0.215).

4.4 Inter-story hysteresis behavior

The inter-story hysteresis of the building show light nonlinear behavior under the synthetic motion SIM81. The maximum inter-story displacements occurred at stories 5 and 6 (Fig. 4.3).

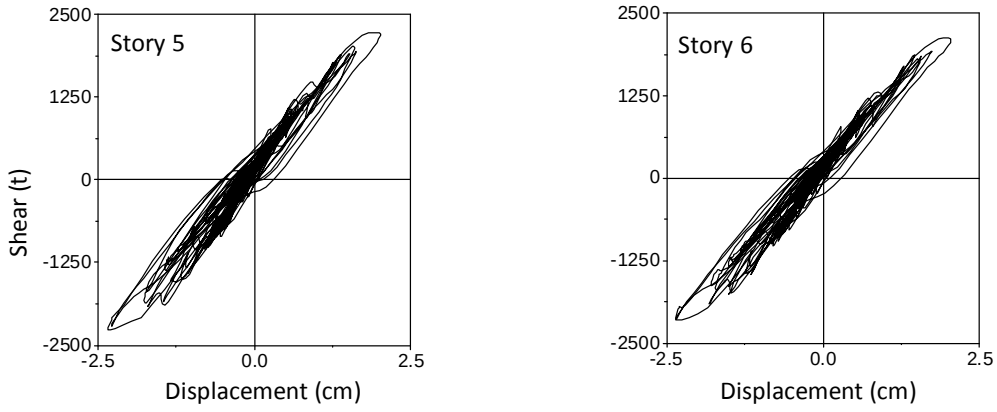

Figure 4.3. Inter-story hysteretic displacements for stories 5 and 6

4.5 Maximum displacements and inter-story drift

The envelope of maximum relative horizontal displacements with respect to the base and the inter-story drift ratio demands are shown in Fig. 4.4. The inter-story drift ratio demands are higher than the design drifts (0.006 given by the local building code, RCMACA, 2002). The design drift is specified in order to limit the damage on non-structural walls. The maximum story drift ratio demand (0.0065) occurred at stories 5 and 6. Based on Alcocer *et al*. (1996), the masonry walls suffer strong strength degradation when the inter-story drifts ratio reaches values of about 0.004 and the stiffness can be degraded up to 15% of the initial stiffness. In other words, the masonry walls resistance and stiffness in this building will be negligible when subjected to strong motion.

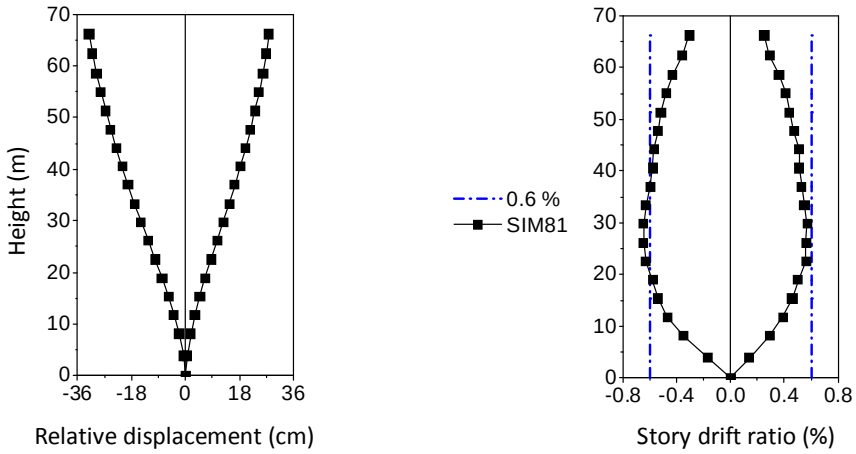

Figure 4.4. Maximum relative displacements with respect to the base and inter-story drift ratio

4.6 Inter-story shear and ductility demand

The inter-story shear demand and design inter-story shear (including load factors) are compared in Fig. 4.5. The inter-story demand exceeds the design values. The design inter-story shear was calculated using the 3D linear model of the building and a spectral analysis. The spectral analysis was performed considering the design spectrum with a seismic coefficient of 0.215, a soil type III, and a Q factor of 4 (RCMACA, 2002).

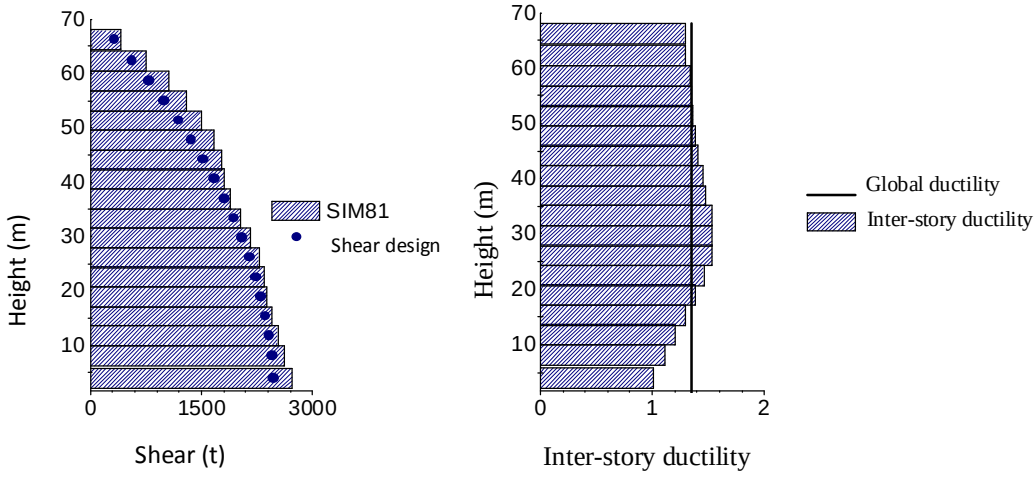

Figure 4.5. Inter-story shear and ductility demand

The inter-story ductility demands (Fig. 4.5) were estimated as a function of yield and maximum displacements presented at each inter-story. The global ductility demand was calculated as the maximum roof displacement divided by the yield displacement. The latter was estimated from an incremental dynamic analysis (IDA)(Vamvatsikos and Cornell, 2002, Montiel *et al*., 2004) and value was 24 cm. The maximum inter-story ductility demands (inter-stories 5 to 7) and the global ductility demand are 1.53 and 1.35, respectively.

4.7 Damage indexes

The damage indexes (DI) have been computed for the building beam members considering the equation by Park and Ang (Park and Ang, 1985 and Carr, 1998):

$$DI = \frac{\mu_m}{\mu_u} + \frac{\beta E_h}{F_y \, \delta_y \mu_u} = \frac{\mu_m}{\mu_u} + \frac{\beta N E_h}{\mu_u} \tag{4.1}$$

where μ_m and μ_u are maximum ductility demand (δ_m/δ_y) and ultimate ductility (δ_u/δ_y), respectively, E_h is the dissipated hysteretic energy, NE_h is normalized energy ($E_h/F_y\delta_y$), β is the structural parameter that characterizes the cycling or cumulative deformation capacity of the element, F_y and δ_y are yield strength and yield displacement, respectively, and δ_u and δ_m are the ultimate and maximum displacements. The positive and negative ultimate ductilities were calculated by the user and provided into the Ruaumoko program. The values of δ_y and δ_m were estimated automatically by the program based on the hysteresis rule parameters used in this study.

Carr and Tabuchi (1993) have indicated that if DI≥1.0, the element fails, if 0.40<DI<1.0, the damage is severe, and if DI≤0.40, the damage is low and the structural element can be repaired. DIs for the frame of building through axis 3 are shown in Fig. 4.6.

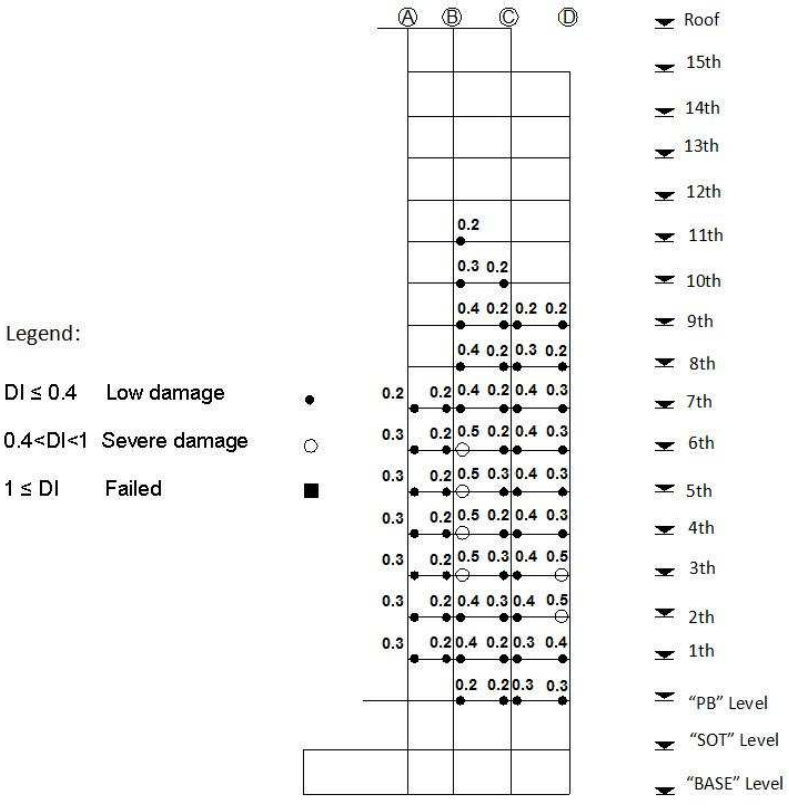

Figure 4.6. Damage indexes at frame through axis 3

5. CONCLUSIONS

The 2D nonlinear response of an instrumented building in Acapulco was studied. The building has been analyzed under the assumption of a strong motion, considering SSI effects and hysteretic behavior of structural elements but ignoring the masonry walls.

The analytical and experimental modal frequencies were calibrated taking into account the assumptions described in detail for the 2D and 3D models.

Because the development of the synthetic ground motion implies uncertainties related to the seismological parameters of empirical Green´s functions and target seismic event, the synthetic records should be considered with caution. In the future, in order to cover these uncertainties, new accelerograms should be developed by using other techniques, for instance different stochastic methods or by spectral matching. Also, it is worthwhile mentioning that the elastic spectra from the synthetic motions exceed that of the spectrum design, particularly for soil type III. Based on these results, the following questions arise: How similar are the synthetic strong ground motions compared to real earthquakes of the Guerrero seismic gap? Is the design spectra obtained from the Acapulco building code suitable? Are there inconsistencies in the building design?

The inter-story shear demands were higher than the design shear. The relative horizontal nonlinear displacements of roof were almost 50% of the linear responses. The nonlinear base shear force obtained is 30% of the linear shear. The maximum seismic coefficient demand, relative displacement roof demand, inter-story drift and inter-story ductility were estimated to be 0.226, 32 cm, 0.65%, and 1.53, respectively.

Finally, based on the available information on the building, the assumptions made, and the synthetic ground motions estimated in this study (Mw=8.2), the nonlinear response showed that some structural elements will suffer severe damage.

ACKNOWLEDGEMENT

This research was funded by DGAPA-UNAM and Federal District Government of Mexico City. The authors wish to thank David Almora, Leonardo Alcántara, Gerardo Castro, Miguel Torres, and Juan M Velasco for the good work carried out in the operation and maintenance of the instrumental networks. We are very grateful to Marco A Macías, Ricardo Pérez and Ricardo Taborda, for their contributions to this research. We acknowledge the helpful comments of Mario Ordaz, and Azekah Griffiths and Thomas Spies for proofreading.

REFERENCES

Alcántara, L., Murià-Vila, D., Almora, D., Velasco, J. M., Torres, M., Vázquez, E. and Macías, M. (2002). Sistema de monitoreo remoto en un edificio localizado en una ciudad expuesta a un peligro sísmico mayor. *Octavas Jornadas Chilenas de Sismología e Ingeniería Antisísmica*. Valparaíso, Chile.

Alcocer, S.M., Murià-Vila, D., Peña, J.I. and Maldonado, J.C. (1996). Comportamiento dinámico de muros de mampostería confinada. *Informe Técnico, Proyecto 5535*. Instituto de Ingeniería, UNAM.

Carr, A.J. (1998). RUAUMOKO computer program library. Department of Civil Engineering. University of Canterbury. New Zealand.

Carr, A.J. and Tabuchi, M. (1993). The structural ductility and the damage index for reinforced concrete structure under seismic excitation. *Proc. Second European Conf. on Struct. Dynamics, EURODYN'93*. Trondheim, Norway.

Kato, D., Otani, S., Katsumata, H. and Aoyama, H. (1983). Effects of wall base rotation behavior of reinforced concrete buildings. *3th South Pacific Conference on Earthquake Engineering*. Wellington, NZ.

Li Xinrong (1995). Reinforced concrete columns under seismic lateral force and varying axial load. *Ph. D Thesis*. Department of Civil Engineering, University of Canterbury.

Montiel, M., Rangel, G., Torres, M. and Ruiz, S.E. (2004). Comparación de la capacidad estructural obtenida

mediante análisis dinámico incremental y análisis estático no lineal. *Memorias XIV Congreso Nacional de Ingeniería Estructural*. Sociedad Mexicana de Ingeniería Estructural, Acapulco, Gro.

Morales-Avilés, W. (2005). Análisis de la respuesta no lineal de un edificio instrumentado en Acapulco. *Master Thesis (In spanish)*. División de Estudios de Posgrado de la Facultad de Ingeniería, UNAM.

Murià-Vila, D., Taborda, R. and Zapata-Escobar, A. (2004). Soil-structure interaction effects in two instrumented tall buildings. *13th World Conference on Earthquake Engineering*. Vancouver, B.C. Canada.

NTC-Concreto (2004). Normas Técnicas Complementarias para Diseño y Construcción de Estructuras de Mampostería. *Gaceta Oficial del Gobierno del Distrito Federal*.

New Zealand Standard (1999). Concrete Structures Standard. The Design of Concrete Structures. NZS 3101:1999. New Zealand.

Ordaz, M., Arboleda, J. and Singh, S.K. (1995). A scheme of random summation of an empirical Green's function to estimate ground motions from future large earthquakes. *Bulletin Seismological Society of America*. **85:6**, 1635-1647.

Otani, S. (1974). SAKE, a computer program for inelastic response of R/C frames to earthquake.. Civil Engineering Studies, Univ. of Illinois at Urbana-Champaign. Report UILU-Eng-74-2029.

Park, Y.J. and Ang, A. (1985). Mechanistic seismic damage model for reinforced concrete. *J. Struct. Div. ASCE*. **111:4**, 722-757.

RCMACA (2002). Reglamento de Construcciones para el Municipio de Acapulco de Juárez, Guerrero. *Honorable Ayuntamiento Constitucional de Acapulco de Juárez 1999-2002*.

Salonikios, T. N., Kappos, A. J., Tegos, I. A., and Penelis, G. G. (1999). Cyclic load behavior of low-slenderness reinforced concrete walls: design basis and test results. *ACI Structural Journal*. **96:4**, 649-660.

Shao-Yeh, M., Bertero, V. and Popov, E. (1976). Experimental and analytical studies on the hysteretic behavior of reinforced concrete rectangular and T-beams. Earthquake Engineering Research Center. University of California, Berkeley. Report No. EERC 76-2.

Singh, S. K. and Mortera, F. (1991). Source-time functions of large Mexican subduction earthquakes, morphology of the Benioff zone and the extent of the Guerrero gap. *J. Geophys. Res.* **96:21**, 487-502.

Taborda, R., Murià-Vila, D., Pérez, R. and Macías, M.A. (2002). Efectos de interacción suelo-estructurade un edificio en Acapulco. *Memorias XIII Congreso Nacional de Ingeniería Estructural*. Puebla, Noviembre.

Tanaka, H. and Park, R. (1990). Effect of lateral confining reinforcement on the ductile behavior of reinforced concrete columns. Department of Civil Engineering. University of Canterbury. Report 90-2.

Vamvatsikos, D. and Cornell, C.A. (2002). Incremental dynamic analysis. *Earthquake Engineering and Structural Dynamics*. **31**, 491-514.

Wang, T. Y., Bertero, V. V., and Popov, E. P. (1975). Hysteretic behavior of reinforced concrete framed walls. Earthquake Engineering Research Center. University of California, Berkeley. Report No. EERC 75-23.

Wilson, E.L. (2000). Three dimensional static and dynamic analysis of structures, a physical approach with emphasis on earthquake engineering. University of California at Berkeley.